

OPTIMIZATION OF PRESSURE RELIEF GROOVES FOR MULTI-QUADRANT HYDRAULIC MACHINES IN DIFFERENT SYSTEM ARCHITECTURES

Thomas Heeger
Linköping University
thomas.heeger@liu.se
Linköping, Sweden

Liselott Ericson
Linköping University
Liselott.ericson@liu.se
Linköping, Sweden

ABSTRACT

In hydraulic axial piston machines, each chamber switches between the high-pressure and the low-pressure port with every revolution. How this process, the commutation, is done, is an essential part of pump design. The commutation typically targets a smooth pressure transition to minimize compressible flow pulsations. However, an ideal pressure match is not possible over the whole operating range of the machine. Thus, pressure relief grooves are considered a “necessary evil” in the state of the art, which can reduce flow pulsations over a wide operating range on the expense of slightly increased losses. Depending on the drive cycle and especially the number of quadrants a hydraulic machine is used in, the optimal pressure relief groove design differs. The increased losses and pulsations for enabling 4-quadrant operation of hydraulic machines are shown. Pump-controlled systems lead to hydraulic machines running in different drive cycles than in conventional valve-controlled systems, affecting ideal groove design. This paper focuses on how to optimize pressure relief grooves and thus presents the methodology incl. the simulation model, formulation of the objective function, and choice of optimization algorithm. Optimizations are carried out for 1-, 2- and 4-quadrant operation. Pareto fronts for a trade-off between flow pulsations and losses are presented, for both a valve-controlled system and a pump-controlled system carrying out the same task in an excavator boom application.

[DOI: <https://doi.org/10.3384/ecp196008>]

Keywords: axial piston pump, multi-quadrant, relief or silencing groove, design optimization

INTRODUCTION

With the ongoing trend towards electrification of hydraulic systems, efficiency and noise become even more important for hydraulic machines. High efficiency is important to reduce required battery size or increase machine uptime, whereas the absence of a combustion engine makes noise from hydraulic machines more audible.

Valve plates play a crucial role for both the efficiency and noise of hydraulic machinery. In the state of the art, pressure relief grooves (also called silencing grooves) are designed to provide a good compromise of efficiency and noise over the whole operating range. Thus, several works have dealt with ideal pressure relief groove design for hydraulic machines.

[1] describes the effect of pressure relief groove design on pump flow ripple and provides analytical equations for relief groove design based on a single operating point. [2] shows possible objectives to quantify noise in hydraulic machines and investigates the formulation of different objective functions. [3] describes a multi-objective optimization of pressure relief grooves in axial piston pumps described by their start and end angles as well as the slope of the opening area over the groove angle. [4] additionally allows non-linear groove area functions. [5] introduces a multi-objective optimization of the opening areas during commutation for a gear pump, followed by a second optimization in which the optimal opening area is approximated by simple geometric features such as circles and triangles.

This work uses multiple operating points to approximate drive cycles for pressure relief groove design. It applies multi-objective optimization on hydraulic machinery which works in 1-, 2- and 4-quadrants. The penalty for 4-quadrant operation is shown. Furthermore, optimizations for the hydraulic machines in two different systems are carried out and compared: a valve-controlled system and a pump-controlled system. The potential for energy recuperation on a system level and the losses and pulsations on a pump-level are quantified based on an exemplary excavator boom application.

VALVE PLATE DESIGN AND PRESSURE RELIEF GROOVES

Hydraulic positive displacement machines can principally work both as a pump and a motor. For the pumping case, displacement chambers are connected to the low pressure (LP) kidney to suck in fluid and the high pressure (HP) kidney to deliver the fluid. In axial piston machines, the kidneys are located in the valve plate. In-between the kidneys, so-called bridges close the displacement chambers and prevent cross-porting (i.e., flow from the HP kidney to the LP kidney through a direct connection provided by the displacement volume) at commutation. Besides separating the inlet channel from the outlet channel, the valve plate needs to provide a smooth pressure transition for each piston chamber. This reduces compressible flow pulsations [6].

For a smooth pressure transition, pre-compression takes place before the displacement volume connects to the HP kidney and de-compression takes place before the displacement volume connects to the LP kidney. Figure 1 shows the principal design for a valve plate for each operating quadrant. As the displacement volume at bottom dead center (BDC) is larger than at top dead center (TDC), the corresponding angle in the valve plate is also larger [7]. The quasi-static pressure change during pre- and de-compression can be calculated as

$$p_{II} - p_I = \beta_e \ln \frac{V_{disp,I}}{V_{disp,II}} \quad (1)$$

with the index I representing the state when entering the bridge and index II representing the state when leaving the bridge. [8]

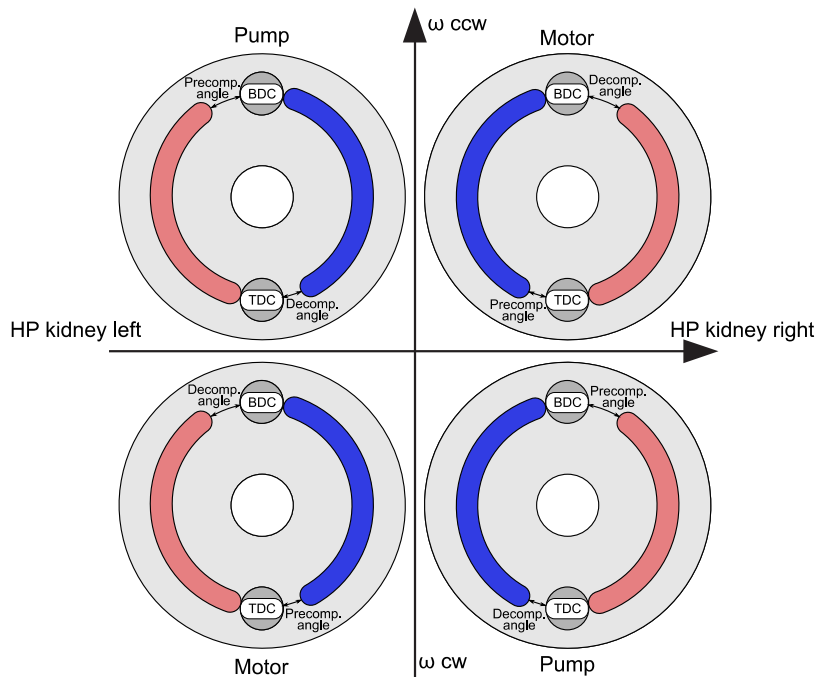


Figure 1 – Principal design of optimized valve plate design for different operating quadrants for a fluid power pump/motor [7].

Equation (1) shows that pre- and decompression angles as shown in Figure 1 can only be customized to one pressure level. For this reason, pressure relief grooves are typically used. Pressure relief grooves are small cuts in the valve plate that provide a small opening between the displacement chamber and the kidneys [9]. The pressure transition is smoothed for a wider range of pressure levels by providing a small channel. However, the flows through the pressure relief grooves lead to undesired losses, so that pressure relief grooves are seen as a "necessary evil" [6].

Palmberg states that pressure relief grooves with quadratically increasing area can provide better results than pressure relief grooves with linearly increasing area and thus the pressure relief grooves in this work are chosen to have a quadratically increasing area. The relative charge time has a dominant effect on the flow pulsations, and therefore the groove area during charging is important. Instead of as a function of time, the groove area can also be expressed as a function of geometry, with A being the orifice area, x being the groove

angle, ω being the shaft frequency, R_b being the cylinder barrel radius and t being the time. For quadratically increasing groove areash. [1]

$$A = k_x \cdot x^n \quad (2)$$

$$x = \omega \cdot R_b \cdot t \quad (3)$$

MODEL-BASED OPTIMIZATION OF PRESSURE RELIEF GROOVES

The following chapter will present a methodology for model-based optimization of pressure relief grooves by discussing the architecture, design variables, objectives and constraints, the simulation model, the choice of operating points and the optimization algorithm used. The process flow is shown in Figure 2.

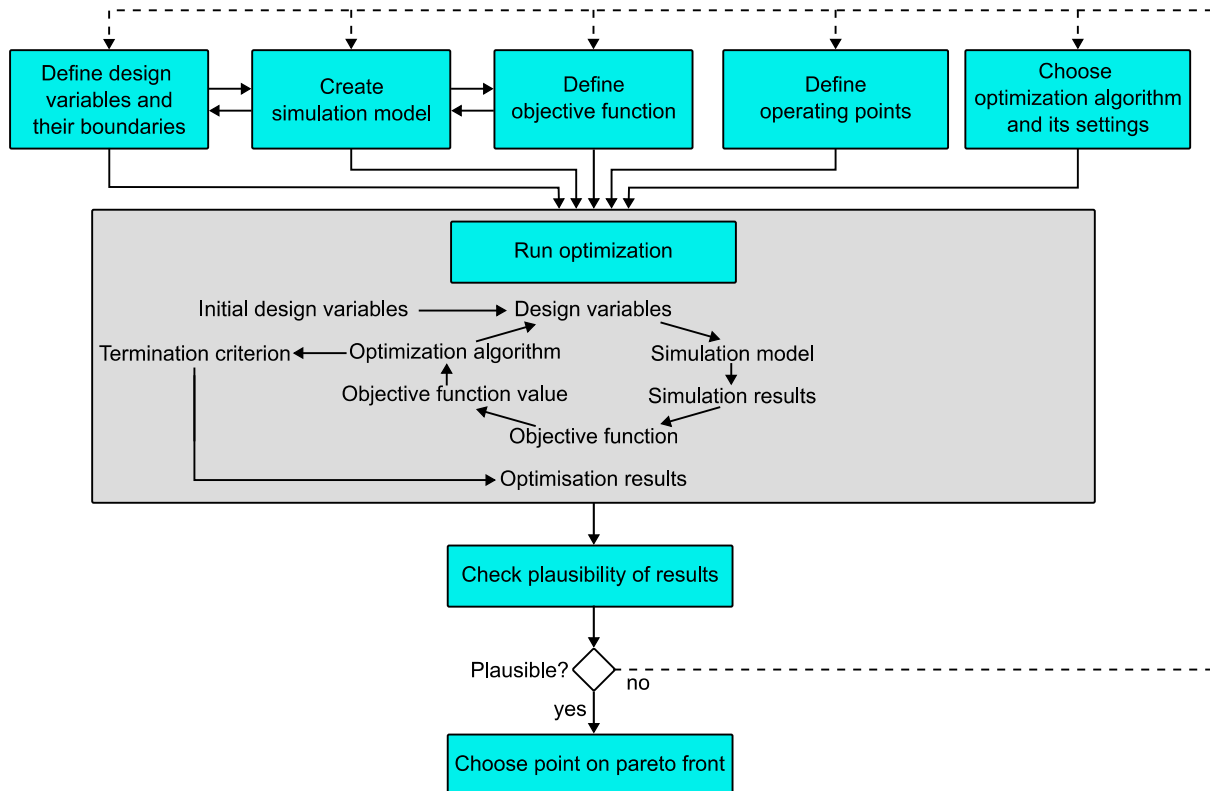


Figure 2 – Process flow of optimization procedure.

Architecture

The optimization algorithm is implemented in MATLAB. The hydraulic machine is simulated in Hopsan. The design variables and simulation time are sent to Hopsan via API, and after the simulation the simulation results are sent to MATLAB as raw data, so that post-processing takes place in MATLAB. The simulation time is always chosen as one period (i.e., the time it takes between two successive pistons pass the same point).

Design Variables

The valve land between the HP kidney and the LP kidney is fixed and covers exactly the angle of one cylinder port opening. At the start and end of each kidney, a pressure relief groove is added. From a manufacturing point of view, each pressure relief groove can be described by the groove angle, the groove shape, and the final area of the groove. As Palmberg [1] stated that grooves with quadratically increasing area can provide better results than pressure relief grooves with linearly increasing area, the groove shape is fixed to a triangular shape with an area that increases quadratically with the groove angle. Cross-porting [9] is not considered in this work to reduce the amount of design variables and thus the computational effort. However, cross-porting could further reduce flow pulsations on the expense of increased losses. The groove angle and the final groove area for each groove are to be optimized. However, there are a lot of

combinations of groove angles and areas that provide poor results due to the interaction of these two parameters. Therefore, k_x (see Equation (2)) replaces the grooves area as design variable, see Figure 3. That means that k_x scales the groove area with the groove angle, and therefore it facilitates the search for an optimal result.

If the machine only operates in 1 or 2 quadrants, only 2 grooves are needed (1 for pre-compression, 1 for de-compression, see Figure 1). In that case, the design variables for the grooves that are not needed might be removed to simplify the problem.

Objectives and Constraints

The objectives and constraints can be defined in a similar way as done in [8]. The objectives are low losses and low noise. In comparison to machines with zero-lapped valve plates, designs that reduce losses typically also reduce noise and vice versa, i.e., the biggest share of loss reduction and noise reduction goes hand in hand. However, for fine-tuning the characteristics, a trade-off between the two objective needs to be made. Pareto fronts are created so that this trade-off between losses and noise can take place a posteriori. As a simplification, the proxy for noise can be peak-to-peak flow pulsations. The LP flow pulsations and the HP flow pulsations are combined to one overall value by weighting them according to their energy content (i.e., their pressure level). To not fully neglect LP flow pulsations for elevated HP levels, a minimum weight for LP flow pulsations can be implemented. However, using peak-to-peak flow pulsations as proxy for noise is a simplification, and more criterions can be used to evaluate noise [2] [4] and the human perception of different frequencies could be taken into account.

The constraints are that a minimum pressure level is to be guaranteed to avoid cavitation and a maximum pressure level is not to be exceeded to avoid excessive mechanical loads. The constraints are implemented as soft constraints.

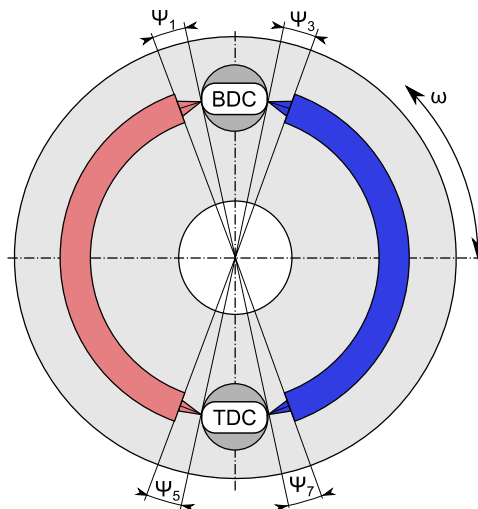


Figure 3 – Sketch of design variables. Each groove is described by its angle (Ψ_1 , Ψ_3 , Ψ_5 and Ψ_7) and its k_x (Ψ_2 , Ψ_4 , Ψ_6 and Ψ_8).

Simulation model

A Hopsan model is used to simulate the steady-state behavior of the pump for pressure relief grooves. Hopsan is a one-dimensional multi-domain simulation tool using the transmission line theory. The structure of the simulation model is illustrated in Figure 4. For each displacement chamber, the model consists of a volume, which is connected to the HP source resp. the LP source through orifices. Each displacement volume is connected to the valve plate, which has two kidneys. At each kidney end, a triangular pressure relief groove is implemented. The valve land between two grooves is the same as for a zero-lapped valve plate. The size of each

displacement volume depends on the shaft angle, and the area and circumference of each orifice depend on the shaft rotation angle.

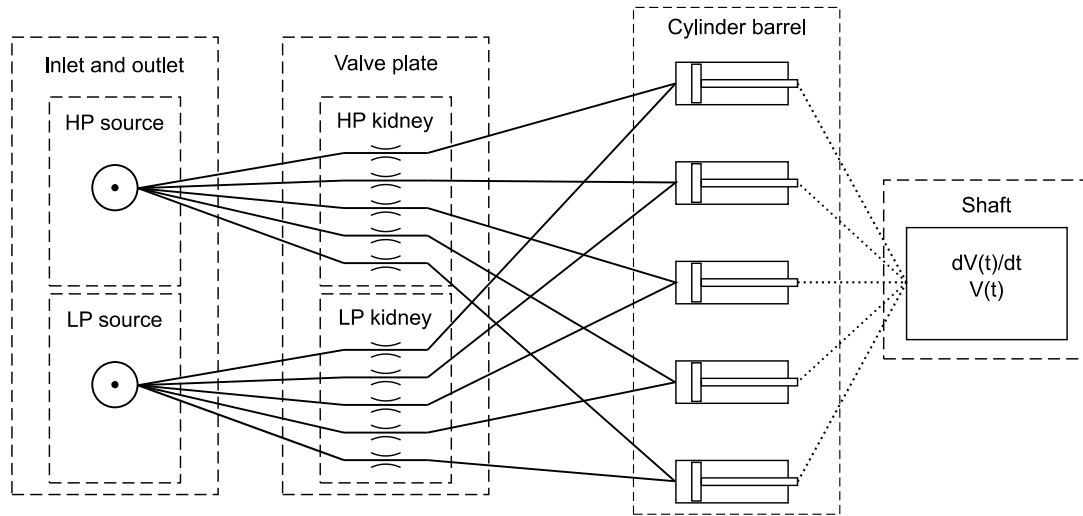


Figure 4 – Illustration of pump model structure. Of course, any number of cylinders can be implemented. [8]

Choice of operating points and trade-off between operating points

Pressure relief grooves are meant to improve the behavior of the hydraulic machine for a wide range of operating points. But the simulation time increases for an increasing number of simulated operating points. Thus, specific operating points need to be selected.

Figure 5 visualizes two different methods of choosing operating points to be considered for optimization. When no drive cycle is available, different pressure and speed levels can be covered with a minimal number of simulations using the Latin Hypercube method [10]. To obtain a 2-quadrant machine, these operating points are additionally “mirrored” with reversed rotational direction of the hydraulic machine as illustrated on the left-hand side of Figure 5. This means that a 2-quadrant machine in this work covers pump and motoring mode by reversing rotational direction, and the pressure sides are not switched. To obtain a 4-quadrant machine, the operating points are additionally appointed with reversed pressure sides of the hydraulic machine.

For a given drive cycle of the hydraulic machine, operating points are clustered into pressure ranges and speed ranges, as exemplary visualized on the right-hand side of Figure 5. The points in the cluster where the machine spends a large amount of time are used as inputs to the optimization. The trade-off between operating points is based on the time spent in each operating point. Thus, the objectives are condensed into average flow pulsations and total losses over the cycle. It is important to consider that losses over a cycle are a more useful objective than efficiencies for specific operating points (e.g., a low efficiency at an operating point with low power might be accepted due to the low absolute losses).

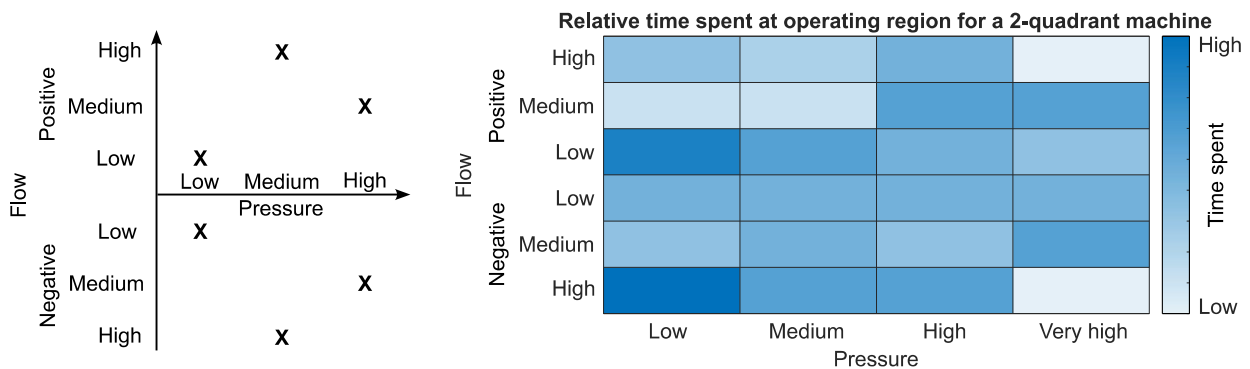


Figure 5 – Choice of operating points on the example of a 2-quadrant machine. Left: Latin Hypercube Method. Right: Clustering of drive cycle data. The data shown here is randomly generated and does not represent a real drive cycle.

Furthermore, operating points which are considered most critical for cavitation are included (i.e., maximum speed, full displacement, and minimum pressure [4]). These operating points are given a low weight, as their performance is not important; however, the constraints are not to be violated for these operating points to guarantee safe operation of the hydraulic machine across its whole operating range.

Choice of optimization algorithm

The Non-dominated Sorting Genetic Algorithm II (NSGA-II) algorithm is used [11]. This algorithm combines the characteristics of individuals and uses mutations to explore the design space. In each generation, new individuals with better objective values can replace individuals with the lower objective values. The Pareto front results from the Pareto-optimal individuals in the last generation.

Exemplary results for 1-, 2- and 4-quadrant machines

The presented methodology has been applied for 1-, 2- and 4-quadrant machines. 3 operating points were chosen for the 1-quadrant machine in pump mode using the Latin Hypercube method. The Pareto fronts are shown in Figure 6 and the corresponding typical valve plate designs are shown in Figure 7. The benefit of an a-posteriori evaluation of the results becomes clear. As the Pareto fronts show, small improvements on one objective can come at a high expense for another objective. The Pareto fronts reveal that the losses and the flow pulsations for the 1- and 2-quadrant machines are on a similar level, i.e., there is no significant penalty for 2-quadrant operation. The 2-quadrant machine even achieves slightly better results, as it uses an additional groove (at Ψ_5) to minimize pulsations due to insufficient pre-compression in motor mode. Due to the decreased pulsations in motor mode, the average pulsations of the 2-quadrant machine can be lower than those of the 1-quadrant machine. Despite this, the typical ideal designs of the 1- and 2-quadrant machine are very similar. However, the Pareto fronts show significantly increased losses and flow pulsations for the 4-quadrant machine. The reason for that can be found in its principal design: to allow for quadrant operation, pressure relief grooves in all 4 possible locations are required (compare Figure 1). However, they need to be significantly shorter than for the 2-quadrant machine, to avoid cavitation. Thus, the 4-quadrant machine has “incomplete” pre-compression and therefore higher losses and pulsations.

It is to be noted that there are some differences between the valve plate designs shown in Figure 7 and typical designs in the state of the art. For the 1- and 2-quadrant machines, there typically also is a groove at Ψ_7 instead of a pure pre-/de-compression. However, as LP flow pulsations receive a very low priority in the objective function, the optimization removes the groove and reduces losses at the expense of increased LP flow pulsations. Furthermore, the groove at Ψ_5 for the 2-quadrant machine is not typical.

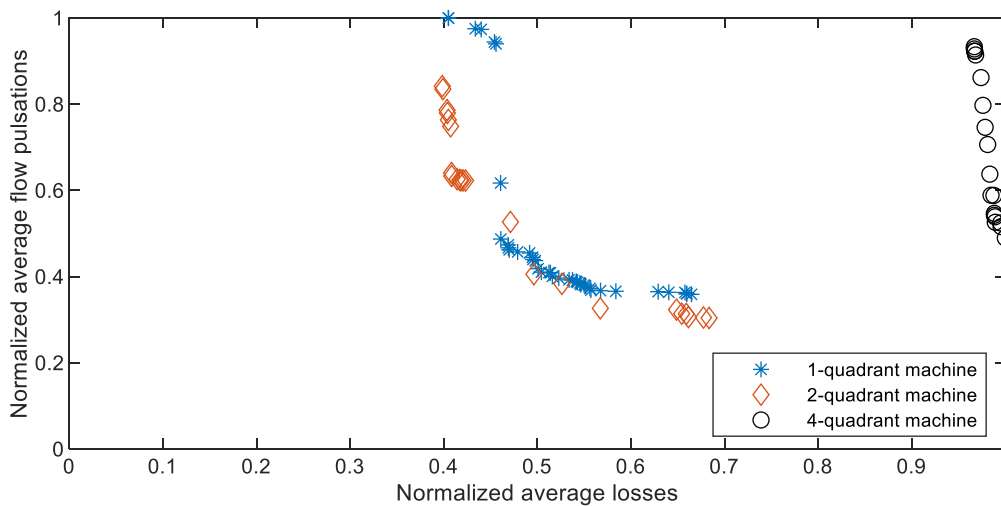


Figure 6 – Pareto fronts for optimized 1-, 2- and 4-quadrant machines

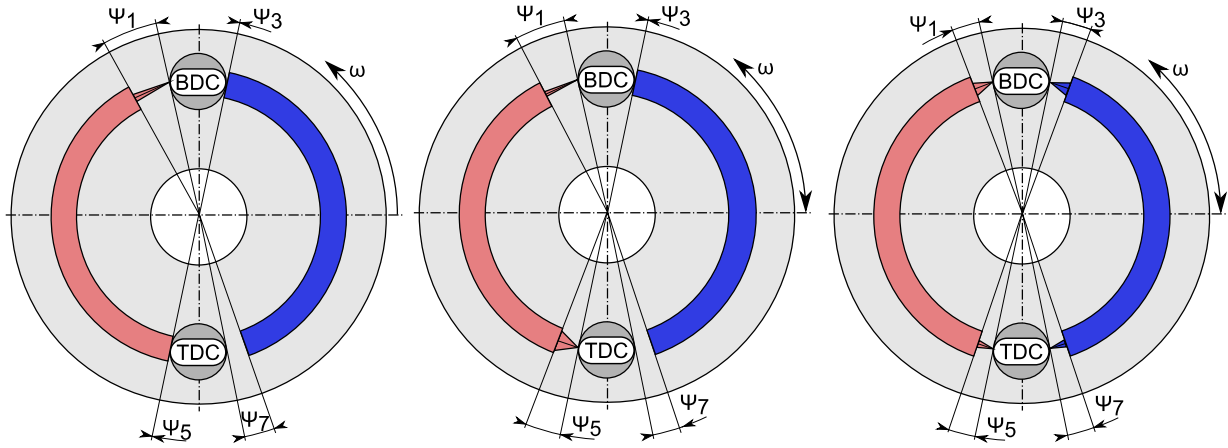


Figure 7 – Qualitative valve plate designs for optimized 1-, 2- and 4-quadrant machines (from left to right)

TRANSLATING REQUIREMENTS FROM 1-QUADRANT MACHINE FOR VALVE-CONTROLLED SYSTEM TO 2- AND 4-QUADRANT MACHINES FOR PUMP-CONTROLLED SYSTEM

Pump-controlled actuators have the potential to contribute to reducing greenhouse gas emissions by reducing throttling losses. Used in electro-hydraulic actuators, they enable energy recuperation [12]. A simple valve-controlled hydraulic actuator system and a pump-controlled system which could replace it are shown in Figure 8. The shown multi-pump system provides more freedom for system control compared to single-pump systems.

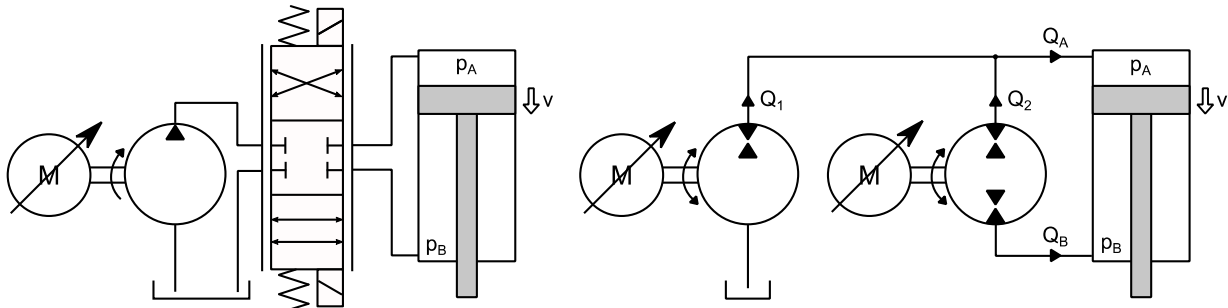


Figure 8 – A valve-controlled system (left) and a possible pump-controlled system (right)

Assuming that the pump-controlled system carries out the same task as the valve-controlled system (i.e., actuator force and speed are identical), the requirements for the hydraulic machines in the pump-controlled system can be deduced from the conventional valve-controlled system. The knowledge on chamber pressures and velocity of the actuator can be a baseline for this.

The actuator shall provide the same force for both systems, see Equation (4). The pump-controlled system's low-pressure is significantly above atmospheric pressure, providing increased stiffness. When both actuator chambers are at this pressure level, the actuator provides a force as calculated in Equation (5). At this force the high-pressure side and the low-pressure side of the actuators switch, providing a smooth transition. Neglecting losses, the pressures for the pump-controlled system are calculated in Equations (6) to (9), and the flows are calculated in Equations (10) to (12). The operating speeds of the hydraulic machines are calculated in Equation (13). With these equations the inputs for the optimization in 2 quadrant and 4 quadrant machines in the pump-controlled system shown in Figure 8 can be calculated and add more detail to a comparison of the pump-controlled system to the valve-controlled system.

$$F_{pc} = F_{vc} = p_{A,vc} \cdot A_A - p_{B,vc} \cdot A_B \quad (4)$$

$$F_{switch} = p_{Low} \cdot (A_A - A_B) \quad (5)$$

$$p_A = p_{Low} , \text{ for } F_{pc} \leq F_{switch} \quad (6)$$

$$p_A = (F_{pc} + p_B \cdot A_B) / A_A , \text{ for } F_{pc} > F_{switch}$$

$$p_B = (p_A \cdot A_A - F_{pc}) / A_B , \text{ for } F_{pc} \leq F_{switch} \quad (7)$$

$$p_B = p_{Low}, \text{ for } F_{pc} > F_{switch}$$

$$\Delta p_1 = p_A - p_{Tank} \quad (8)$$

$$\Delta p_2 = p_A - p_B \quad (9)$$

$$Q_A = v \cdot A_A, Q_B = -v \cdot A_B \quad (10)$$

$$Q_1 = Q_A - Q_2 = v \cdot (A_A - A_B) \quad (11)$$

$$Q_2 = -Q_B \quad (12)$$

$$n_{1,2} = Q_{1,2}/V_{1,2} \quad (13)$$

EXEMPLARY RESULT FOR EXCAVATOR BOOM APPLICATION

Equations (4) to (13) were applied on a drive cycle for an excavator boom application. For the sizing of the hydraulic machines, it was assumed that they all possess the same maximum speed, and then their displacements were chosen according to the maximum flow that passes the machine. For the given drive cycle, the 1-quadrant machine runs at maximum speed when filling the A-side of the cylinder, whilst the 2-quadrant and 4-quadrant machine run at maximum speed when the A-side is vented.

Table 1 shows the displacements and powers of the hydraulic machines. The pump-controlled system requires an increase of the total installed displacement and power. The advantage of the pump-controlled system becomes obvious: whilst the average input power (in pump mode) is only slightly elevated, a large amount of power is available for recuperation, thus offering great potential for increased system efficiency.

Table 1 – Displacement and average power of the hydraulic machines

	1-quadrant machine	2-quadrant machine	4-quadrant machine
Displacement [cm ³ /rev]	42.0	29.9	35.3
Total average power [kW]	18.6	15.3	16.1
thereof pump mode [kW]	18.6	9.9	10.5
thereof motor mode [kW]	0	5.4	5.5

Figure 9 shows exemplary Pareto fronts when optimizing the hydraulic machines for equivalent cycles for the system shown in Figure 8. Despite the increased average power running through the hydraulic machines for the pump-controlled system, the combined total losses are on a similar level. Concerning flow pulsations, note that each machine was optimized individually, i.e., the flow pulsations of one machine were not used as input to another machine. When assuming that the peak-to-peak flow pulsations of the machines for the pump-controlled systems are summated, they are still at a similar level to the valve-controlled system's machine. However, in practice both machines will run at different speeds. Thus, the flow pulsation will occur at different frequencies and the worst case of peaks of both machines being aligned with one another will rarely happen.

Furthermore, it is to be noted that the drive cycle was taken from an excavator boom application, which rarely switches the direction of force on the cylinder. Thus, the optimization of the 4-quadrant machine yielded in a design which is a mixture of the typical design for 2- and 4-quadrant machines: while there are no grooves (or extremely short grooves) at Ψ_3 and Ψ_5 (typical for 2-quadrant machines), the grooves at Ψ_1 and Ψ_7 have a smaller angle to avoid cavitation (typical for 2-quadrant machines). For a different application which switches pressure sides more often, e.g., an excavator arm, a design more typical to the classical 4-quadrant design as shown in Figure 7 is to be expected, and thus the 4-quadrant machine will have higher levels of flow pulsations and losses.

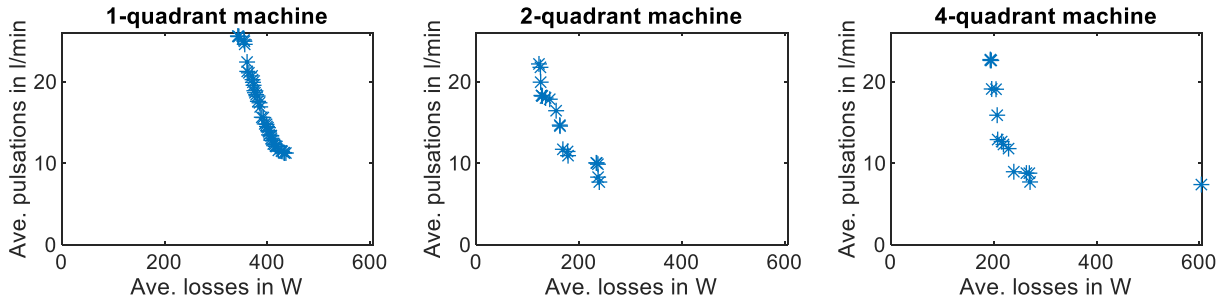


Figure 9 – Pareto fronts for optimized machines for excavator boom drive cycle

CONCLUSION

A methodology for pressure relief groove optimization has been presented and applied on machines for 1-, 2- and 4-quadrant operation and their general designs have been shown. The penalty for enabling 4-quadrant operation has been shown. Furthermore, the methodology has been applied on hydraulic machines for a valve-controlled system and a pump-controlled system on the example of an excavator boom drive cycle. The optimization results show that despite the large potential for energy savings on a system level and the higher average power passing through the hydraulic machines, there is no significant penalty in terms of losses or flow pulsations when using a pump-controlled system.

ABBREVIATIONS

HP	High-pressure
LP	Low-pressure

NOMENCLATURE

k_x	Groove area constant [m^2/rad^n]
n	Exponent in groove area function [-]
n_i	Speed of hydraulic machine i [rev/s]
$p_{I,II}$	Pressure in displacement chamber before / after bridge [Pa]
Δp_1	Pressure difference over pump 1 [Pa]
Δp_2	Pressure difference over pump 2 [Pa]
p_A	Pressure in cap side of cylinder [Pa]
p_B	Pressure in rod side of cylinder [Pa]
p_{Low}	Pressure in cylinder's low-pressure side [Pa]
p_{Tank}	Pressure in tank line [Pa]
t	Time [s]
v	Cylinder velocity [m/s]
x	Groove angle [rad]
A_A	Cylinder cap end area [m^2]
A_B	Cylinder rod end area [m^2]
F_{pc}	Force in pump-controlled system [N]
F_{switch}	Force at which high-pressure side of cylinder is switched [N]
F_{vc}	Force in valve-controlled system [N]
Q_1	Flow through hydraulic machine 1 [m^3/s]
Q_2	Flow through hydraulic machine 2 [m^3/s]
Q_A	Flow into cap side of cylinder [m^3/s]
Q_B	Flow into rod side of cylinder [m^3/s]
R_b	Cylinder barrel radius [m]
$V_{disp,I,II}$	Displacement volume before / after bridge [m^3]
V_i	Displacement of hydraulic machine i [m^3/rev]

β_e	Fluid's bulk modulus [1/Pa]
ω	Shaft speed [rad/s]
$\Psi_{1,3,5,7}$	Design variables for groove angles [rad]
$\Psi_{2,4,6,8}$	Design variables for groove area constants [m ² /rad ⁿ]

ACKNOWLEDGMENTS

This research was funded by the Swedish Energy Agency (Energimyndigheten, Grant Number 50181-1).

REFERENCES

- [1] J. O. Palmberg, "Modelling of flow ripple from fluid power piston pumps," in 2nd Bath International Power Workshop, University of Bath, UK, 1989.
- [2] L. Ericson, J. Ölvander and J.-O. Palmberg, "On optimal design of hydrostatic machines," in Proceedings of the 6th International Fluid Power Conference, IFK, Vol WS, 2008.
- [3] G. K. Seeniraj and M. P. Ivantysynova, "A Multi-Parameter Multi-Objective Approach to Reduce Pump Noise Generation," International Journal of Fluid Power, vol. 12, pp. 17-7, 2011.
- [4] P. K. Kalbfleisch and M. Ivantysynova, "Computational Valve Plate Design in Axial Piston Pumps/Motors," International Journal of Fluid Power, September 2019.
- [5] S. Gulati and A. Vacca, "A General Method to Determine the Optimal Profile of Porting Grooves in Positive Displacement Machines: the Case of External Gear Machines," in 10th International Fluid Power Conference (10. IFK), Dresden, Germany, 2016.
- [6] N. D. Manring, Fluid Power Pumps and Motors: Analysis, Design and Control, McGraw Hill Book CO, 2013.
- [7] L. Ericson, S. Kärnell and M. Hochwallner, "Experimental Investigation of a Displacement-controlled Hydrostatic Pump/Motor by Means of Rotating Valve Plate," in Proceedings of 15:th Scandinavian International Conference on Fluid Power, (SICFP'17), Linköping, Sweden, 2017.
- [8] T. Heeger and L. Ericson, "A New Degree of Freedom for Variable Axial Piston Pumps with Valve Plate Rotation," in Proceedings of the 17:th Scandinavian International Conference on Fluid Power, SICFP21, June 1-2, 2021, Linköping, Sweden, 2021.
- [9] T. Kim, P. Kalbfleisch and M. Ivantysynova, "The effect of cross porting on derived displacement volume," International Journal of Fluid Power, vol. 15, p. 77–85, May 2014.
- [10] M. D. McKay, R. J. Beckman and W. J. Conover, "A Comparison of Three Methods for Selecting Values of Input Variables in the Analysis of Output from a Computer Code," Technometrics, vol. 21, p. 239, May 1979.
- [11] K. Deb, S. Agrawal, A. Pratap and T. Meyarivan, "A fast and elitist multiobjective genetic algorithm: NSGA-II," IEEE Trans. Evol. Comput., vol. 6, pp. 182-197, 2002.
- [12] S. Ketelsen, D. Padovani, T. O. Andersen, M. K. Ebbesen and L. Schmidt, "Classification and Review of Pump-Controlled Differential Cylinder Drives," Energies, vol. 12, 2019.